

Ultrasonic Bonding of Ag Ribbon on Si Wafers With Various Backside Metallization

Meng-Ting Chiang, National Taiwan University, Taiwan

Pei-Ing Lee, National Taiwan University, Taiwan

Ang-Ying Lin, National Taiwan University, Taiwan

Tung-Han Chuang, National Taiwan University, Taiwan*

ABSTRACT

Ultrasonic ribbon bonding has gained much attention due to the endeavor of achieving higher module performance in power electronic packaging. Among all the ribbon materials, Ag ribbon is a promising candidate due to its superior electrical properties. However, research which has reported the bonding of the ribbon on chip side is scant. Thus, in this study, the authors carried out bonding of the Ag ribbon on various types of metallized wafers to examine the feasibility of Ag ribbon, simulating the bonding scenario on the chip side in power modules. Results revealed that bonding of the Ag ribbon is feasible on those wafers metallized Ag on top. The authors also discussed the implications for the bondability of Ag ribbon with different types of metallization layers.

KEYWORDS

Ag Ribbon, Bonding Strengths, Si Wafer Backside Metallization, Ultrasonic Bonding

INTRODUCTION

Semiconductor chips are connected electrically to other components or systems in order to function. Such electrical connections are critical to electronic packaging and are accomplished by utilizing various forms of conductors to build up the signal or power connection pathways within a single package. Therefore, the bonding should provide a decent electrical interconnection that will not decay with time, while providing excellent performance of the semiconductor chips. Wire bonding is one of the standard interconnection techniques for electrically connecting microchips to the terminal of a chip package or directly to a substrate (Harman, 2010). Generally, the wire bonding technology can either be categorized by the wire bonding method (ball–wedge or wedge–wedge) or the bonding mechanism that creates the metallic interconnection between wire and substrate (thermo-compression, ultrasonic or thermosonic) (Jung et al., 2019).

Each bonding method entails a range of advantages and drawbacks; therefore, the decision to use one of them has to be made with consideration of the application. A recent industry survey has shown that about 90% of all electronics packages and assemblies are made of ball bonds, while the rest are produced with wedge bonds. The most established material for bond wire is gold alloy (>

DOI: 10.4018/IJMMME.333626

*Corresponding Author

This article published as an Open Access article distributed under the terms of the Creative Commons Attribution License (<http://creativecommons.org/licenses/by/4.0/>) which permits unrestricted use, distribution, and production in any medium, provided the author of the original work and original publication source are properly credited.

90% Au), usually doped with elements such as beryllium to increase the strength and ductility so as to improve properties such as wire loop height, elongation at break, temperature strength, breaking load or tensile strength (Simons et al., 2000). Meanwhile, different types of bond wires have been designed to adapt to technological niches such as high-current applications, assemblies restricted to low processing temperatures, or bonds with enhanced mechanical strength. Some common bond wires are aluminum wire, palladium coated copper wire, and silver-alloy wires. The wire sizes are typically 0.6 to 2 mils; however, for power devices, larger diameter wires ranging from 5 to 20 mils in diameter are used for a higher current carrying capacity (Zhou et al., 2023). Thermosonic bonding enhances the reliability of previous mechanisms by preheating the bonding wire in advance of the ultrasonic cycle to reduce cracking issues in Si chips. As an alternative to thermocompression bonding, thermosonic bonding has been broadly used for Au gold wire bonding of ICs in both packages and multichip modules. In power electronic packaging, however, most of the wire diameters are around 300–500 μm due to the high voltage and current applied (Liu, 2012). The formation of the ball bond in the thermosonic bonding method becomes rather tricky when the wire diameter increases, and this challenge has given rise to efforts to achieve bonding through ultrasonic bonding (Maeda & Takahashi, 2013). Ultrasonic bonding can be used to join a wide variety of metals (Neppiras, 1965), rendering it a popular bonding technique today. However, the operation requires careful handling to prevent mechanical damage, and the acoustical properties of the joining materials can change causing variations in strength.

As for wire materials, metals with high electrical conductivity and a high diffusion rate, such as Cu (Lim et al., 2014), Au (Wulff et al., 2003), Ag (Chen et al., 2022), and Al (Schneider-Ramelow & Ehrhardt, 2016), are commonly used for wire bonding. Among these metals, gold wire is a very attractive choice because this metal is fully utilized in ultrasonic, mechanical force, and heat processes. Moreover, Au wire is profoundly electrically conductive, almost a significant degree more so than other metals. Au has much higher oxidation resistance than other metals and is relatively soft, which is important for delicate surfaces.

The characteristics of Cu are very similar to those of Au. Cu wire bonding was the first option adopted to replace Au wire bonding in semiconductor packaging. The great interest in Cu is driven by its lower cost, better electrical resistivity, and tool readiness. Cu wire bonding has been implemented in recent nano-scale semiconductor packaging in industry due to its conductivity properties and cost effectiveness (Chauhan et al., 2013; Zhou et al., 2023). Cu wire began to emerge in the mid-1990s and was not initially deployed in large scale manufacturing due to its vulnerability to wire corrosion and oxidation (Xu et al., 2009). Currently, many researchers are dedicated to studying the reliability issues of copper wires (Lim et al., 2021; Mathew et al., 2022; Qin et al., 2019). As a solution to the drawbacks of Cu wire bonding, different types of Cu alloys have been introduced since 2010, some examples being Pd-doped or Pd-coated Cu wires for various applications and humidity reliability performance (Clauberg et al., 2010.). Despite this limited use, Cu wire bonding is not an ultimate bonding wire solution for advanced power module packaging due to its intrinsic material hardness, which could cause chip cratering during ultrasonic bonding (Gross et al., 2016). This drawback has led to the widespread usage of Al wire.

Similar to Au and Cu, Al has low electrical resistance, making it suitable for interconnections among the components of electronic packaging (Schneider-Ramelow & Ehrhardt, 2016). Al wires can also be used for conductive interconnections, but only ultrasonic energy and mechanical force play key roles in shaping the Al bond. It is noteworthy that Al allows interconnections to be constructed on temperature-susceptible materials, as it does not demand the high temperature conditions generally required for Au and Cu wire bonding. Furthermore, Al is utilized in most of chip metallization. Al wire is likewise very desirable for bonding on chip surfaces to form homogeneous bonding interfaces, which are highly correlated to the joint integrity of wire bonds. However, the low melting point and poor mechanical properties of Al have limited its usage in some applications, especially in power electronics with high reliability demands, leading to a new search for wire materials.

Since the 2010s, Ag wire bonding has been widely introduced in chip-scale packages and light emitting diode semiconductor packaging (Chuang et al., 2020; Lan et al., 2013; Tsai et al., 2013). Recent studies have evaluated the feasibility of Ag and Ag-alloy as the next candidates for wire alloys to replace conventional Au and Cu bonding wire (Guo et al., 2015; Tsai et al., 2016; Zhou et al., 2020). With the increasing power level demands of power electronic packaging, Ag-alloy wire material could be a feasible choice for interconnection bonding in power modules.

Furthermore, a new trend of utilizing ribbon to replace heavy wire has gained much attention due to the lower resistance, large cross-section, and better reliability of ribbon (Chen et al., 2020; Heimann et al., 2012; Jacques et al., 2015), which shows superior performance in comparison to traditional heavy wires in reliability tests and therefore is favored for special packaging structures (Heimann et al., 2012). For ribbon bonding application in high power modules, there have been numerous studies related to Al ribbon, Al-Cu ribbon, and Cu ribbon bonding (Delmonte et al., 2023; Li et al., 2023; Lu et al., 2023; Nwanoro et al., 2018) However, there has been relatively limited exploration in the area of Ag and Ag alloy ribbon bonding; only a few studies have reported the feasibility and process parameters (Chen & Chuang, 2020; Chen & Chuang, 2021; Chen & Chuang, 2022). The difficulty lies in the fact that the bonding process of heavy ribbon on the chip side requires increased ultrasonic energy to soften the ribbon material, presenting a high possibility of chip cratering during bonding. Therefore, more precise process parameter design is required for the bonding of ribbon on the chip side, and the design of the wafer metallization layer should also be considered.

This paper supplements the findings of the authors' earlier study (Chen & Chuang, 2022). It is similar to the previous study of Ag-alloy ribbon, which was successfully bonded on direct bonded copper substrates, in that the focus of this study is on the bonding of Ag ribbon on metallized wafer, which simulates the chip-side interconnection of a power module. It differs from previous studies in that the bondability of the Ag ribbon on various types of metallized wafers is assessed. The metallization systems bonded with Ag ribbon described here could serve as the basis for a study of Ag ribbon bonding on the top side of the chip in power modules.

EXPERIMENTAL

The Ag ribbon in this study was produced from 6 mm Ag rods with a chemical composition of 99.99% Ag, which was prepared by vacuum induction melting through continuous casting in an oven. The 6 mm metal rod was subsequently drawn to 2.6 mm and annealed at 530 °C for 3 h to release the accumulated stress from cold working, after which it was drawn to a diameter of 437 μm and rolled into a ribbon with a thickness of 100 μm and width of 1500 μm. The microstructure of the Ag ribbon was characterized by electron backscatter diffraction (EBSD). The Ag ribbon was then bonded on Si wafers with metallization layers of Ti/Ni, Ti/Ni/Cu, Ti/Ni/Cu/Ag, and Ti/Ni/Ag to evaluate the bondability. The equipment used for the ultrasonic bonding was an Asterion™ Wedge Bonder (Kulicke & Soffa), and Table 1 shows the bonding parameters. The authors obtained these parameters in their previous study as the ideal parameters for ultrasonic bonding. They subsequently cross-sectioned and polished the bonded samples with 0.3 μm alumina suspension, and observed the bonding interface by scanning microscopy.

RESULTS AND DISCUSSION

Microstructure of the Ag Ribbon

In power electronic packaging, the main goal of ultrasonic ribbon bonding is to reach a trade-off balance between the process workability and the quality of the bonds. Better understanding of the Ag ribbon material from the microstructural point of view is crucial because the physical properties of the ribbon material appear to be highly dependent on its microstructure. The authors discussed the

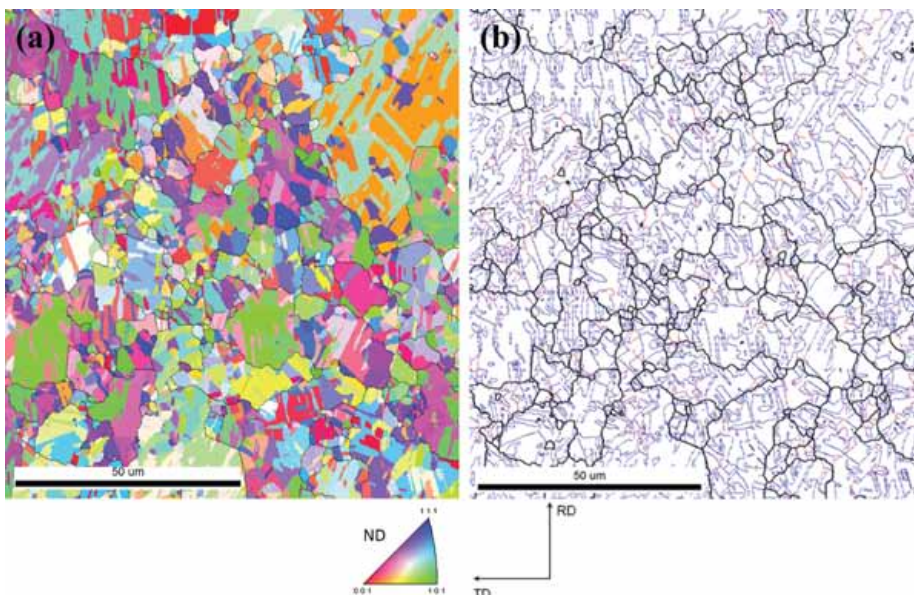
Table 1. Bonding parameters of Ag ribbon on wafer metallization

Heading	Heading
Touch force (cN)	4000
Start force (cN)	3000
Bond force (cN)	4000
Start power (digit)	100
Bond power (digit)	120
Loop length (mm)	10
Loop height (mm)	2

grain growth and twin formation in Ag-alloy ribbon in their previous study (Chen et al., 2021), but have not reported the microstructure of pure Ag ribbon, yet. Figure 1 presents the inverse pole figure of the as-manufactured Ag ribbon, which exhibited a great number of annealing twins (colored in blue as $\Sigma 3$ and in red as $\Sigma 9$) within the normal grain boundaries (colored in black). It is known that the ultrasonic bonding mechanism is dominated by the microslip model together with deformation of the surface and the relative motion at the bonding interfaces (Lum et al., 2006). Such a microstructure of Ag ribbon could have significant effects during bonding with different types of metallized wafers. The next section provides the authors' evaluation of the bondability of the Ag ribbon with different metallized wafers.

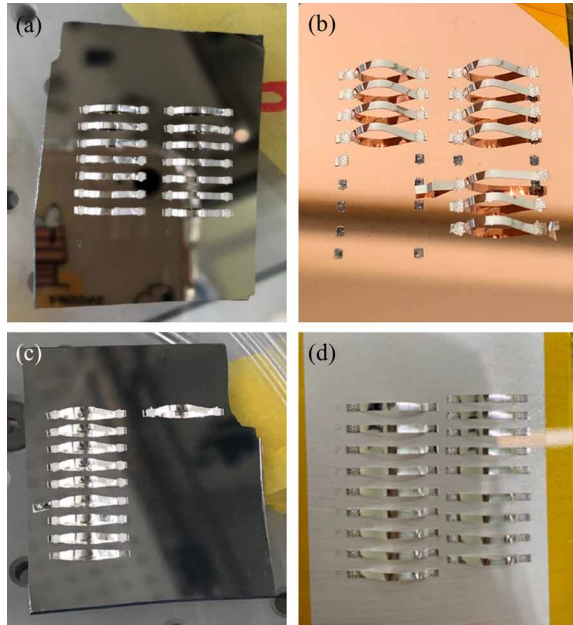
The Ag ribbon was bonded on Si wafers with metallization layers of Ti/Ni, Ti/Ni/Cu, Ti/Ni/Cu/Ag, and Ti/Ni/Ag, the bonded samples of which are in Figure 2(a)-(d), respectively. As Figure 2(a) shows, Ag ribbon seemed to be successfully bonded on the Ti/Ni metallized wafer; however, the

Figure 1. EBSD mapping of Ag ribbon: (a) inverse pole figure map; (b) grain boundary characterization with twin boundary distribution (black line: normal grain boundaries; blue line: $\Sigma 3$ twin boundaries; red line: $\Sigma 9$ twin boundaries)



Bondability of Ag Ribbon on Ti/Ni, Ti/Ni/Cu, Ti/Ni/Cu/Ag, and Ti/Ni/Ag Metallized Wafers

Figure 2. Ultrasonic bonding of Ag ribbons on Si wafer metallized with (a) Ti/Ni, (b) Ti/Ni/Cu, (c) Ti/Ni/Cu/Ag, and (d) Ti/Ni/Ag



overall bonding performance was not ideal. The adhesion of most of the contact points was weak. Some of these points were directly peeled off the wafer during the ultrasonic bonding process. The successfully bonded contact points exhibited severe deformation attributed to the bonding process, which would have an adverse effect on the strength of the bonding interface.

On the other hand, the yield rate of Ag ribbon bonded on Ti/Ni/Cu metallized wafers was lower than that of Ti/Ni samples (Figure 2(b)); in fact, only 50% of the bonds were successful. Some of the ribbon bonds were peeled off, and the metallization layers were directly pulled off along with the wedge bond joints. The authors preliminarily speculated that the Ti/Ni/Cu metallization layer was unable to withstand such a high bond force during ultrasonic bonding and failed as a tear failure at the localized area of the adhesion joint.

In the case of the Ti/Ni/Cu/Ag metallized wafer (Figure 2(c)), however, ribbon wedge bonds were successfully adhered on the metallization surface with no observable failures at the two joints. The yield rate of the bond was 100%, with no peeling of the metallization layer or cratering of the silicon. The better bonding performance of the Ti/Ni/Cu/Ag wafer metallization system implied that the Ag film had relatively better compatibility with Ag ribbon than those of Ni and Cu. The authors observed a similar bonding condition in the case of Ti/Ni/Ag wafer (Figure 2(d)). This was consistent with the good bondability shown in the Ti/Ni/Cu/Ag system, in which two metallization systems comprised an Ag layer on the top surface and were bonded with the Ag ribbons. The results indicated that bonding of the Ag ribbon on the chip side required Ag as the top metallization layer to improve the bondability. The following discussion focuses on the interfacial morphology of the bonded joints specifically relevant to the relation between the metallization layer and the ribbon.

Interfacial Analysis of Ag Ribbon Bonding on Metallized Wafers

A successful ultrasonic bond requires a sound contact layer with intact metallization. Any damage to the substrate during the bonding process could degrade the reliability of the bonding interface. Therefore, the bonding interfaces were further examined with polished cross-sections and scanning microscopy images. Figures 3 and 4 present the cross-sectional interfaces of the first and second

Figure 3. Cross-sectional images of the interfaces of Ag ribbon bonded Si wafers metallized with (a) Ti/Ni, (b) Ti/Ni/Cu, (c) Ti/Ni/Cu/Ag, and (d) Ti/Ni/Ag at first bond

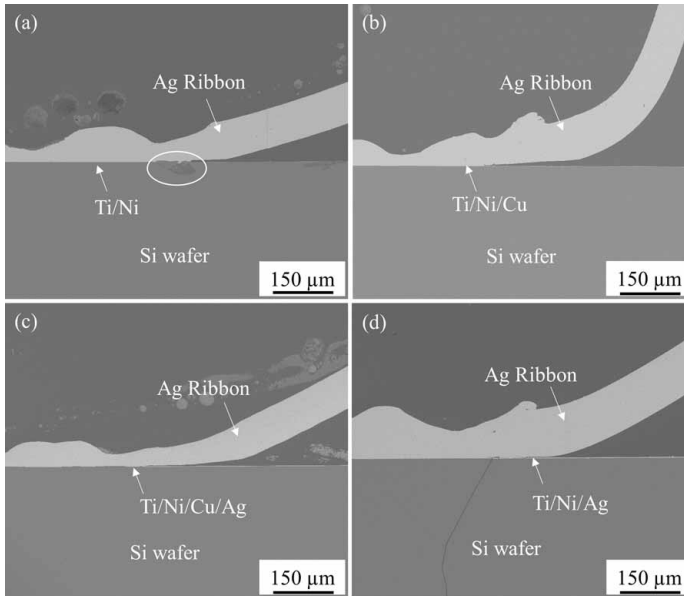
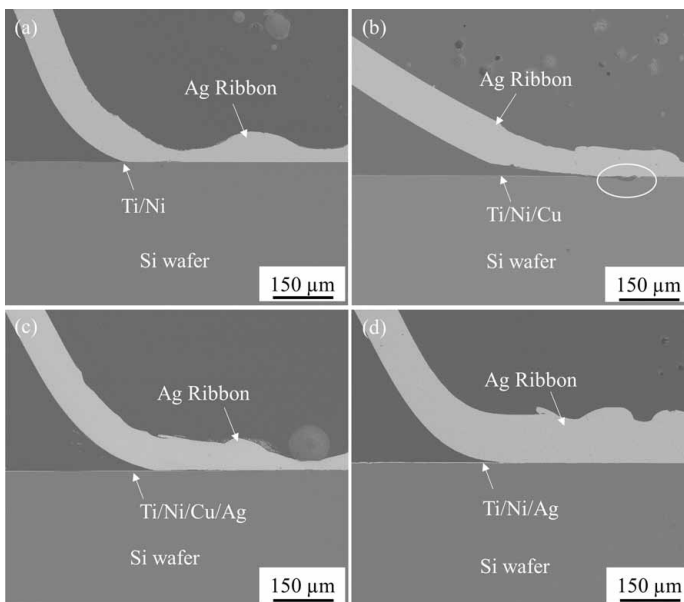


Figure 4. Cross-sectional images of the interfaces of Ag ribbon bonded Si wafers metallized with (a) Ti/Ni, (b) Ti/Ni/Cu, (c) Ti/Ni/Cu/Ag, and (d) Ti/Ni/Ag at second bond



bonds of Ag ribbons bonded with different types of backside metallized wafers, respectively. As indicated by circles in Figure 3(a) and Figure 4(b), the researchers observed cracks in the first and second bonds of the samples of Ag ribbon bonded with Ti/Ni and Ti/Ni/Cu metallized wafers. They attributed this cracking to the high ultrasonic energy applied to the Ag ribbon during the bonding

process. However, in the bonds with Ti/Ni/Cu/Ag, and Ti/Ni/Ag layers, the cross-sectional images revealed flat and continuous interfaces with intact metallization layers. The laminations of the interfaces were distinct and the authors found no cracks within them, indicating successful bonding and the absence of severe cratering.

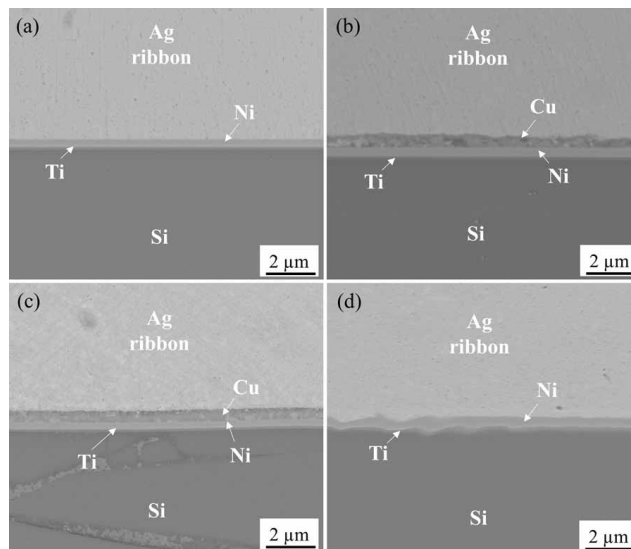
The bonding strengths of the Ag ribbons ultrasonically bonded on Si wafers metallized with various thin films were measured with both pull and shear tests. As Table 2 shows, the shear strengths were slightly higher than the results of pull tests. The authors also found that the Ti/Ni/Cu/Ag metallized Ag ribbon joint had optimized pull and shear strengths, while those of the ultrasonic bonds of Ag ribbon on Si wafers metallized with traditional Ti/Ni/Ag were acceptable. In contrast, both the Si/Ti/Ni and Si/Ti/Ni/Cu metallized Si wafers showed relatively low pull and shear strengths after ultrasonic bonding with Ag ribbon.

The above results can be interpreted from the metallurgical point of view. In ultrasonic bonding, the applied ultrasonic energy can initiate the welding of two metal surfaces together at localized surface irregularities (Neppiras, 1965). The metallic surfaces go through a series of adhesion and friction processes, which result in metal fatigue and interdiffusion at the interface, rather than the formation of intermetallic compounds. As Figure 5 illustrates, the magnified interfaces of the Ag ribbon bonded with Ti/Ni, Ti/Ni/Cu, Ti/Ni/Cu/Ag, and Ti/Ni/Ag metallized wafers showed distinct layered structures, with no intermetallic compounds.

Table 2. Average pull strengths and shear strengths for Ag ribbons ultrasonically bonded on Si wafers with different backside metallization layers; bonding parameters of ag ribbon on wafer metallization

Si backside Metallization Layers	Pull Strength (kgf)	Shear Strength (kgf)
Si/Ti/Ni	0.44	0.33
Si/Ti/Ni/Cu	0.39	0.63
Si/Ti/Ni/Cu/Ag	1.39	1.73
Si/Ti/Ni/Ag	1.25	1.28

Figure 5. Magnified interfacial images at the bonded regions of Ag ribbon with Si wafers metallized with (a) Ti/Ni, (b) Ti/Ni/Cu, (c) Ti/Ni/Cu/Ag, and (d) Ti/Ni/Ag layers



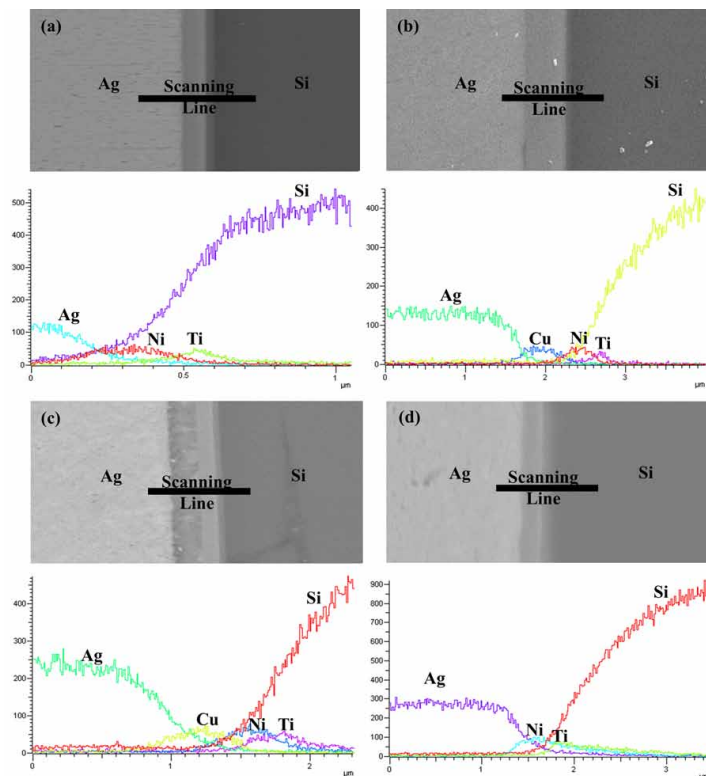
Therefore, the crystallographic difference of the Ag ribbon with the wafer metallization layers may explain the successful bonding. Table 3 reports the crystal structures of the metals involved in the ribbon material and wafer metallization layers. The metals the authors utilized in this study all had the FCC crystal structure and were categorized in the Fm-3m space group. However, these metals have different cell parameters, and greater cell parameter differences could cause larger lattice mismatch. Certainly, if a Ag metallization layer is utilized, it will have no lattice mismatch with Ag ribbon. In contrast, the large mismatch between Ag and the elements Cu and Ni could be the culprit behind the unsuccessful bonds. Based on the above discussion, it could be expected that metals with closer cell parameters are likely to have a higher possibility of being welded together owing to the smaller lattice mismatch.

Of particular interest to this study was the bonding interface. The interfaces of the Ag ribbon and the metallized wafers were examined by EDS line scan (Figure 6). Unlike conventional Al ribbon, which entails issues with intermetallic compounds, Ag raised only diffusion concerns. According to

Table 3. Atomic properties of the metallization layers and ribbons (Chen et al., 2020)

Material	Crystal Structure	Space Group	Cell Parameter
Ag	FCC	Fm-3m	a=b=c=408.53 pm
Cu	FCC	Fm-3m	a=b=c=361.47 pm
Ni	FCC	Fm-3m	a=b=c=352.40 pm

Figure 6. EDS line scans of bonding interfaces of Ag ribbon with Si wafers metallized with (a) Ti/Ni, (b) Ti/Ni/Cu, (c) Ti/Ni/Cu/Ag, and (d) Ti/Ni/Ag layers



the binary phase diagram of Ag with Ni and Cu, they have limited solubility with one another, for Ni and Cu are not solid soluble in Ag at low temperatures. No interdiffusion of Ag-Ni and Ag-Cu occurred, indicating that no solid solution formed at the interface. This was consistent with the line scans, in which no overlapping was observed across the Ag/Cu or Ag/Ni interfaces. In other words, the bonding interfaces were composed of distinct layers of metal films. Importantly, in the case of Ag ribbon on metallization layers of Ti/Ni/Ag and Ti/Ni/Cu/Ag, the interfaces between the ribbon material and the top Ag layers of the metallization were not distinct because of the interdiffusion of the Ag ribbon and Ag metal film. Apparently, this diffusion process facilitated the bonding, as the interfacial images in Figure 2 and Figure 3 indicate.

As ultrasonic bonding is developed for more advanced applications in the electronic packaging industry, the control of process stresses induced on the integrated circuits increases in importance. Therefore, the feasibility of Ag ribbon bonding on Al or Cu metallized metal-oxide-semiconductor field-effect transistor and insulated gate bipolar transistor power semiconductors is a crucial concern for designing future generations of power modules. In this study, the authors investigated the prototypical packaging scenarios and relevant interconnections to pave the way for future system designs. The evaluation of the feasibility of bonding Ag ribbon on the chip side showed that wafers with Ag as the top metallization layer could achieve better bondability. Ag ribbon is a promising candidate and a reliable option for high-power IC packages; however, further optimization of the bonding parameters, ribbon material, and metallization technique is necessary to achieve high quality ribbon bonds on different types of substrates to accommodate a wide range of applications.

CONCLUSION

Based on the successful experience of replacing Au wires, the authors consider Ag and Ag alloy ribbons as viable options for high-power ICs. In this study, the authors demonstrated the feasibility of bonding Ag ribbon on various kinds of metallization layers on Si wafer. The results showed that ultrasonic bonding of Ag ribbon is feasible with a metallization structure comprising Ag as the top surface. In contrast, bonding with Cu and Ni metallization layers on the surface showed poor bondability, which was explained from the metallurgical point of view as the combined result of crystallographic mismatch and the low solid solubility of the contact metals. The observed interfacial images presented the great possibility of bonding Ag ribbon with Ti/Ni/Cu/Ag and Ti/Ni/Ag metallization systems, in that the interfaces were free of gaps and cratering issues. The authors' research results indicate the substantial potential of using Ag ribbon for top-side interconnections, which can meet the high-performance requirements of power modules. Therefore, this study holds significant guidance in providing feasible solutions for electronic packaging.

ACKNOWLEDGMENT

The results in this paper are based on the Ph.D. thesis of one of the co-authors (Dr. Pei-Ing Lee) from National Taiwan University; the thesis is available in the library but has not yet been published elsewhere. This study was sponsored by the Emerging Technology Application Program of the Hsinchu Science Park R&D program of Ag Materials Technology Co., LTD, under Grant No. 112AO03A.

REFERENCES

- Chauhan, P., Zhong, Z. W., & Pecht, M. (2013). Copper wire bonding concerns and best practices. *Journal of Electronic Materials*, 42(8), 2415–2434. doi:10.1007/s11664-013-2576-1
- Chen, C. H., & Chuang, T. H. (2022). Optimization of Ag-alloy ribbon bonding: An approach to reliable interconnection for high power IC packaging. *Microelectronics and Reliability*, 137(August), 114786. doi:10.1016/j.microrel.2022.114786
- Chen, C. H., Lai, Y. C., & Chuang, T. H. (2021). Grain growth and twin formation in a Ag-4Pd alloy ribbon after annealing treatments. *Journal of Alloys and Compounds*, 863, 158619. doi:10.1016/j.jallcom.2021.158619
- Chen, C. H., Lee, P. I., & Chuang, T. H. (2022). Microstructure evolution and failure mechanism of electromigration in Ag-alloy bonding wire. *Journal of Alloys and Compounds*, 913, 165266. doi:10.1016/j.jallcom.2022.165266
- Chen, C. H., Lin, Y. C., Groth, A., Lai, Y. C., Lin, C. Y., Chang, H. M., & Chuang, T. H. (2020). Ultrasonic bonding of Ag and Ag-alloy ribbon: An innovative alternative for high power IC packages. *IEEE Transactions on Components, Packaging, and Manufacturing Technology*, 10(6), 1061–1068. doi:10.1109/TCPMT.2020.2988129
- Chuang, T. H., Lee, P. I., & Lin, Y. C. (2020). An optimized Ag-5Pd-3.5Au bonding wire for the resistance of Ag ion migration in LED packages. *IEEE Transactions on Components, Packaging, and Manufacturing Technology*, 10(12), 1989–1995. doi:10.1109/TCPMT.2020.3034213
- Clauberg, H., Chylak, B., Wong, N., Yeung, J., & Milke, E. (2010). Wire bonding with Pd-coated copper wire. In *Proceedings of the 2010 IEEE CPMT Symposium Japan* (pp. 1-4). IEEE.
- Delmonte, N., Santoro, D., Provenzale, L., & Cova, P. (2023). Investigating failure mode and mechanism of copper ribbon interconnections in operating photovoltaic modules. *Microelectronics and Reliability*, 150, 115094. doi:10.1016/j.microrel.2023.115094
- Gross, D., Haag, S., Reinold, M., Schneider-Ramelow, M., & Lang, K. D. (2016). Heavy copper wire-bonding on silicon chips with aluminum-passivated Cu bond-pads. *Microelectronic Engineering*, 156, 41–45. doi:10.1016/j.mee.2015.12.017
- Guo, R., Gao, L., Li, M., Mao, D., Qian, K., & Chiu, H. (2015). Microstructure evolution of Ag-8Au-3Pd alloy wire during electromigration. *Materials Characterization*, 110, 44–51. doi:10.1016/j.matchar.2015.10.009
- Harman, G. (2010). *Wire bonding in microelectronics*. McGraw-Hill Education.
- Heimann, M., Klaerner, P., Luechinger, C., Mette, A., Mueller, J. W., Traeger, M., Barthel, T., Valentin, O., & Wawer, P. (2012). Ultrasonic bonding of aluminum ribbons to interconnect high-efficiency crystalline-silicon solar cells. *Energy Procedia*, 27, 670–675. doi:10.1016/j.egypro.2012.07.127
- Jacques, S., Leroy, R., & Lethiecq, M. (2015). Impact of aluminum wire and ribbon bonding technologies on D2PAK package reliability during thermal cycling applications. *Microelectronics and Reliability*, 55(9–10), 1821–1825. doi:10.1016/j.microrel.2015.06.012
- Jung, D. Y., Cain, S. R., & Chen, W. T. (2019). Introduction to wire bond technology. In *Encyclopedia of packaging materials, processes, and mechanics* (pp. 1–21). doi:10.1142/9789811209666_0001
- Lan, A., Tsai, J., Huang, J., & Hung, O. (2013). Interconnection challenge of wire bonding - Ag alloy wire. In *Proceedings of the 2013 IEEE 15th Electronics Packaging Technology Conference, EPTC 2013* (pp. 504–509). doi:10.1109/EPTC.2013.6745771
- Li, Y., Hassan, M., Wu, Y., Emon, A. I., Deng, S., Luo, F., Deshpande, A., & McKeown, M. (2023). A comprehensive evaluation of al heavy wire bonding and ribbon bonding application in high power WBG power modules. *IMAPSource Proceedings*, 2022(1), 000010–000017. doi:10.4071/001c.74596
- Lim, A. B. Y., Chang, A. C. K., Yauw, O., Chylak, B., Gan, C. L., & Chen, Z. (2014). Ultra-fine pitch palladium-coated copper wire bonding: Effect of bonding parameters. *Microelectronics and Reliability*, 54(11), 2555–2563. doi:10.1016/j.microrel.2014.05.005
- Lim, M. J. Z., Goroll, M., Loh, H. G., Chen, Z., & Tan, C. S. (2021). Copper wire degradation under high temperature and high humidity without molding compound. In *Proceedings of the 2021 IEEE 23rd Electronics Packaging Technology Conference (EPTC)* (pp. 440–444). IEEE. doi:10.1109/EPTC53413.2021.9663891

- Liu, Y. (2012). Power electronic packaging. In *Power Electronic Packaging* (1st ed.). Springer New York. doi:10.1007/978-1-4614-1053-9
- Lu, P., Li, L., Lu, G. Q., Shuai, Z., Guo, X., & Mei, Y. H. (2023). Review of double sided cooling power modules for driving electric vehicles. *IEEE Transactions on Device and Materials Reliability*, 23(2), 287–296. doi:10.1109/TDMR.2023.3272928
- Lum, I., Mayer, M., & Zhou, Y. (2006). Footprint study of ultrasonic wedge-bonding with aluminum wire on copper substrate. *Journal of Electronic Materials*, 35(3), 433–442. doi:10.1007/BF02690530
- Maeda, M., & Takahashi, Y. (2013). Ultrasonic bonding of aluminum and copper wires in power electronics. In *Proceedings of the 1st International Joint Symposium on Joining and Welding* (pp. 511–515). Elsevier. doi:10.1533/978-1-78242-164-1.511
- Mathew, V., Chopin, S. F., Li, G., & Xu, S. (2022). Post wirebonding coating for prevention of corrosion of wire bonded packages by chlorine containing foreign particles. In *Proceedings of the 2022 IEEE 72nd Electronic Components and Technology Conference (ECTC)* (pp. 495-501). IEEE. doi:10.1109/ECTC51906.2022.00084
- Neppiras, E. A. (1965). Ultrasonic welding of metals. *Ultrasonics*, 3(3), 128–135. doi:10.1016/S0041-624X(65)80003-8
- Nwanoro, K. C., Lu, H., Yin, C., & Bailey, C. (2018). An analysis of the reliability and design optimization of aluminium ribbon bonds in power electronics modules using computer simulation method. *Microelectronics and Reliability*, 87, 1–14. doi:10.1016/j.microrel.2018.05.013
- Qin, W., Anderson, T., & Chang, G. (2019). Mechanism to improve the reliability of copper wire bonding with palladium-coating of the wire. *Microelectronics and Reliability*, 99, 239–244. doi:10.1016/j.microrel.2019.04.010
- Schneider-Ramelow, M., & Ehrhardt, C. (2016). The reliability of wire bonding using Ag and Al. *Microelectronics and Reliability*, 63, 336–341. doi:10.1016/j.microrel.2016.05.009
- Simons, C., Schräpler, L., & Herklotz, G. (2000). Doped and low-alloyed gold bonding wires. *Gold Bulletin*, 33(3), 89–96. doi:10.1007/BF03215484
- Tsai, C.-H., Chuang, C.-H., Tsai, H.-H., Lee, J.-D., Chang, D., Lin, H.-J., & Chuang, T.-H. (2016). Materials characteristics of Ag-alloy wires and their applications in advanced packages. *IEEE Transactions on Components, Packaging, and Manufacturing Technology*, 6(2), 298–305. doi:10.1109/TCPMT.2015.2453410
- Tsai, H.-H., Chuang, T.-H., Lee, J.-D., Tsai, C.-H., Wang, H.-C., Lin, H.-J., & Chang, C.-C. (2013). High performance Ag-Pd alloy wires for high frequency IC packages. In *Proceedings of the 2013 8th International Microsystems, Packaging, Assembly and Circuits Technology Conference (IMPACT)* (pp. 162–165). doi:10.1109/IMPACT.2013.6706697
- Wulff, F., Breach, C. D., & Dittmer, K. (2003). Crystallographic texture of drawn gold bonding wires using electron backscattered diffraction (EBSD). *Journal of Materials Science Letters*, 22(19), 1373–1376. doi:10.1023/A:1025751714880
- Xu, H., Liu, C., Silberschmidt, V. V., Pramana, S. S., White, T. J., & Chen, Z. (2009). A re-examination of the mechanism of thermosonic copper ball bonding on aluminium metallization pads. *Scripta Materialia*, 61(2), 165–168. doi:10.1016/j.scriptamat.2009.03.034
- Zhou, H., Chang, A., Fan, J., Cao, J., An, B., Xia, J., Yao, J., Cui, X., & Zhang, Y. (2023). Copper wire bonding: A review. *Micromachines*, 14(8), 1612. doi:10.3390/mi14081612 PMID:37630148
- Zhou, H., Zhang, Y., Cao, J., Su, C., Li, C., Chang, A., & An, B. (2023). Research progress on bonding wire for microelectronic packaging. *Micromachines*, 14(2), 432. doi:10.3390/mi14020432 PMID:36838134
- Zhou, W. Y., Pei, H. Y., Luo, J. Q., Wu, Y. J., Chen, J. L., Kang, F. F., Kong, J. W., Ji, X. Q., Yang, G. X., & Yang, A. H. (2020). Influence of Pd content on microstructure and performance of Au-coated Ag alloy wire. *Journal of Materials Science Materials in Electronics*, 31(8), 6241–6247. doi:10.1007/s10854-020-03178-0